ISSN 0021-3640, JETP Letters, 2017, Vol. 105, No. 1, pp. 26–33. © Pleiades Publishing, Inc., 2017.

CONDENSED MATTER

Magnetic Phase Separation and Strong Enhancement of the Néel Temperature at High Pressures in a New Multiferroic $Ba_3TaFe_3Si_2O_{14}$[1]

I. S. Lyubutin[a]*, S. S. Starchikov[a, b], A. G. Gavriliuk[a, b, c], I. A. Troyan[a, b, c], Yu. A. Nikiforova[a, b], A. G. Ivanova [a, b], A. I. Chumakov[d, e], and R. Rüffer[d]

[a] *FSRC "Crystallography and Photonics," Russian Academy of Sciences, Moscow, 119333 Russia*

[b] *Institute for Nuclear Research, Russian Academy of Sciences, Troitsk, Moscow, 142190 Russia*

[c] *REC "Functional Nanomaterials," Immanuel Kant Baltic Federal University, Kaliningrad, 236041 Russia*

[d] *European Synchrotron Radiation Facility, CS40220, F-38043, Grenoble, France*

[e] *National Research Center Kurchatov Institute, Moscow, 123182 Russia*

***** *e-mail: lyubutinig@mai.ru*

Received November 18, 2016

The high-pressure properties of a new multiferroic of the langasite family $Ba_3TaFe_3Si_2O_{14}$ were investigated in diamond-anvil cells (DAC) in the temperature range of 4.2–295 K by a new method of synchrotron Mossbauer spectroscopy. Strong enhancement of the Néel temperature T_N was observed at pressures above 20 GPa associated with the structural transformation. The highest value of T_N is about 130 K which is almost five times larger than the value at ambient pressure (about 27 K). It was suggested that the high value of T_N appears due to redistribution of Fe ions over $3f$ and $2d$ tetrahedral sites of the langasite structure. In this case, the short Fe-O distances and favorable Fe-O-Fe bond angles create conditions for strong superexchange interactions between iron ions, and effective two-dimensional (2D) magnetic ordering appears in the (ab) plane. The separation of the sample into two magnetic phases with different T_N values of about 50 and 130 K was revealed, which can be explained by the strong 2D magnetic ordering in the (ab) plane and 3D ordering involving inter-plane interaction.

DOI: 10.1134/S0021364017010027

1. INTRODUCTION

The iron-containing compound $Ba_3TaFe_3Si_2O_{14}$ is a representative of a large family of langasite ($La_3Ga_5SiO_{14}$) crystals, which are famous by their unique piezoelectric, laser and nonlinear optical properties [1, 2]. Recently, the langasite-type compounds containing magnetic $3d$ ions have attracted a great interest as a new type of multiferroics [3–10]. The crystal structure of langasite belongs to the non-centrosymmetric trigonal structure of the $Ca_3Ga_2Ge_4O_{14}$ type with space group $P321$ and $Z = 1$ [11].

Iron ions in $Ba_3TaFe_3Si_2O_{14}$ occupy the $3f$ tetrahedral sites. The tetrahedral layers containing Fe^{3+} and Si^{4+} ions are in the ab plane, and are separated along the c axis with the layers consisting of oxygen octahedra (Ta^{5+}) and large dodecahedra (Ba^{2+}). The Fe^{3+} ions form a net of triangle clusters on a hexagonal lattice in the ab planes creating the triangle magnetic structure with frustrated interactions [3, 6]. The neutron diffraction studies of the similar crystal $Ba_3NbFe_3Si_2O_{14}$ [3, 5] revealed the 120°—ordering of Fe magnetic moments in the ab plane at low temperatures. In addition, the magnetic vector rotates from layer to layer (in the ab plains), when alternating along the c axis, thus forming a helical magnetic structure [3]. Crystallographic and magnetic chirality was recently studied in the iron-containing langasites experimentally [12–14] and theoretically [7, 15, 16].

Splitting of crystallographic iron sites into two sublattices was found by the transmission Mössbauer spectroscopy (TMS) in the $Ba_3TaFe_3Si_2O_{14}$ and $Ba_3NbFe_3Si_2O_{14}$ compounds at ambient pressure [4, 6], which was associated with the structural phase transition induced by the magnetic ordering below Néel temperature $T_N = 27.2$ K. The appearance of nonequivalent Fe^{3+} sites can be explained by the struc-

[1] The article is published in the original.

tural transition $P321 \rightarrow P3$ (or $P321 \rightarrow C2$) induced by the magnetic transition [6].

Recent XRD studies of $Ba_3TaFe_3Si_2O_{14}$ at high pressures P revealed two structural phase transitions at P of about 5.5 and 20 GPa [17]. At the first transition, a shift of light oxygen atoms increases the local symmetry $3f$ oxygen tetrahedra occupied by iron. At the second transition, the unit cell volume drops abruptly by 8.6% while the c unit cell parameter is greatly decreased. It was proposed that the significant reduction of the c parameter should lead to a substantial increase in the exchange interaction between iron ions in adjacent planes (ab), which can lead to an increase in the Néel point of this crystal at pressures above 20 GPa [17, 18].

In the present study, polycrystalline langasite $Ba_3TaFe_3Si_2O_{14}$ samples were investigated under high pressures in a diamond-anvil cell (DAC) [19] by a new method of synchrotron Mössbauer spectroscopy (SMS) [20–22] in the temperature range of 4.2–295 K and at pressures from ambient to 30 GPa. At $P >$ 20 GPa the separation of the sample into magnetic and nonmagnetic phases was observed above 30 K. The estimated value of Néel temperature of the magnetic phase is highly increased relative to ambient pressure value, however the fraction (volume) of the magnetic phase decreases with the temperature at the expense of the nonmagnetic fraction.

2. EXPERIMENTS

Polycrystalline $Ba_3TaFe_3Si_2O_{14}$ samples were synthesized by the ceramic technology from the oxides and salts of the starting components [1]. For Mössbauer study, iron in the samples was enriched with ^{57}Fe isotope to 50 wt %. X-ray powder diffraction confirmed the phase composition of $Ba_3TaFe_3Si_2O_{14}$ with the unit cell parameters $a = 8.538(2)$ Å and $c = 5.237(2)$ Å [1]. From the low-temperature Mössbauer measurements by the traditional transmission Mössbauer spectroscopy methodic (TMS), the Néel temperature of this compound was found to be $T_N = 27.2(\pm 0.1)$ K [4].

For the high pressures experiments, the sample was located in a DAC [19]. The cullet diameter of diamond anvils was about 250 μm and the hole diameter in the rhenium gasket was about 100 μm. The powder sample was molded between diamond anvils to form a plate of about 6 μm thick, and 25×25 μm in plane and mounted within the chamber. In an optical microscope, the plate appeared to the eye as a transparent dark yellow object. Helium was used as the best quasi-hydrostatic pressure-transmitting medium, which ensured the minimum pressure gradient in the sample. The pressure was determined and controlled by the standard ruby fluorescence technique.

In order to study the magnetic properties of $Ba_3TaFe_3Si_2O_{14}$ at high pressures and low temperatures the new technique of SMS at ^{57}Fe nuclei was applied [21, 22]. In this method, synchrotron radiation is used instead of radioactive ^{57}Co source in the TMS technique, which is commonly used in the laboratory. The SMS spectra are recorded in energy representation (as well as the TMS spectra), which differs SMS from another synchrotron Mössbauer methodic of nuclear resonance forward scattering (NFS) where spectra are recorded in the time domain mode. The spectra processing and analysis that is well developed for the energy-domain TMS spectroscopy can be applied to the SMS spectra. Meanwhile, in contrast to the TMS technique, the processing of the SMS spectra requires the software that uses the full transmission integral calculation and a normalized squared Lorentz shape of the source line.

The measurements were performed at the Nuclear Resonance beamline ID18 [21] at the European Synchrotron Radiation Facility (ESRF) in Grenoble, France. Mössbauer spectra for $Ba_3TaFe_3Si_2O_{14}$ were measured using Synchrotron Mössbauer Source (SMS) [22].

X-rays with the energy of 14.4 keV were premonochromatized to the bandwidth of ~2 eV by high-heat-load monochromator. Further monochromatization down to the energy bandwidth of ~100 meV was achieved with a high-resolution monochromator. Finally, the beam was reflected by a high-quality iron borate $^{57}FeBO_3$ crystal in pure nuclear (111) reflection. Temperature of the crystal was kept few tens of a degree above the Néel temperature (75.8°C). Under these conditions, the crystal reflects only the X-rays in the vicinity of the Mössbauer nuclear resonance with the energy spectrum of a single-line with the bandwidth of about two natural widths of the nuclear resonance transition.

The beam was then focused by a Kirkpatrick–Baez mirror to a spot size of about 30 μm. The intensity of the beam at the sample position was $\sim 1.0 \times 10^4$ photons per second. The X-ray beam was directed along the DAC axis, perpendicular to the sample plane. The velocity scale of the Mössbauer spectra was calibrated using α-Fe foil. The isomer shift cited in this work is given relative to the α-Fe spectrum at ambient conditions. During measurements, the source line width before and after collecting each Mössbauer spectrum of the sample was controlled using a single-line standard Mössbauer absorber $K_2Mg^{57}Fe(CN)_6$ with an intrinsic line width of 0.21 mm/s.

Mössbauer spectra for $Ba_3TaFe_3Si_2O_{14}$ were measured for several pressures up to 30 GPa in a temperature range from 4.2 to 295 K for each pressure point. The data treatment was performed using the MossA software package [23].

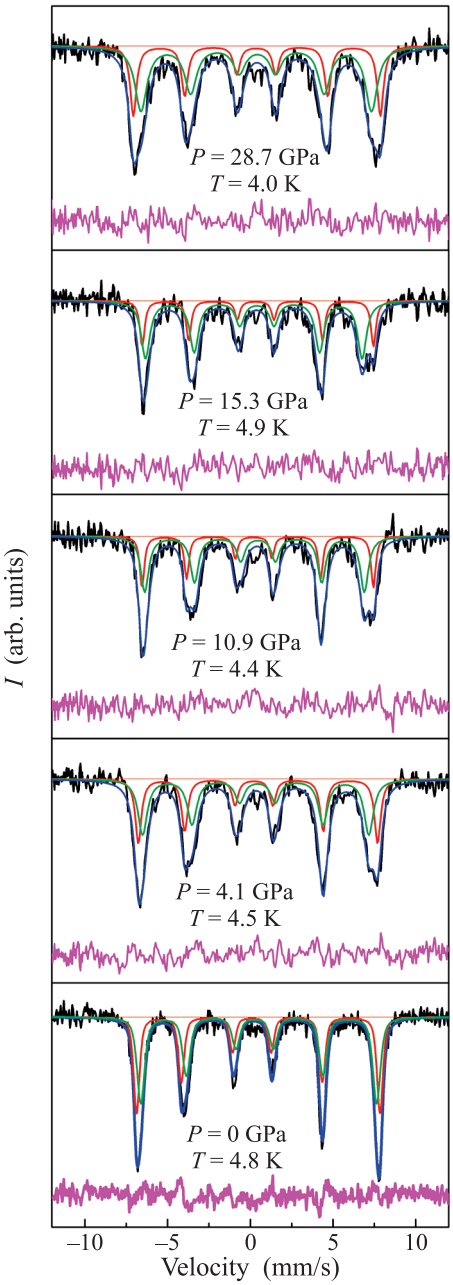

Fig. 1. (Color online) SMS spectra of $Ba_3TaFe_3Si_2O_{14}$ at liquid helium temperature and different pressures up to $P = 29$ GPa. Solid lines are the calculated subspectra for two non-equivalent iron sites fitted to the experimental data.

3. EXPERIMENTAL RESULTS

At the lowest temperature of 4.0–4.9 K, the SMS spectra are split into six resonance lines demonstrating magnetic ordering of Fe ions at all pressures (Fig. 1).

The spectra can be well fit with two magnetic components, which correspond to two non-equivalent sites of iron ions. Such an effect (splitting of the $3f$

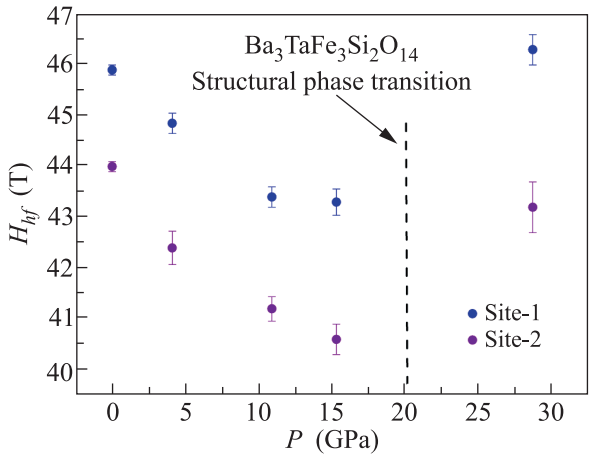

Fig. 2. (Color online) Pressure dependence of magnetic hyperfine fields at iron ions in two non-equivalent iron sites of $Ba_3TaFe_3Si_2O_{14}$ at liquid helium temperature. The dashed line separates the data below and above the structural phase transition at $P = 20$ GPa.

sites) was first observed in $Ba_3TaFe_3Si_2O_{14}$ at ambient pressure, and it was associated with the structural phase transition induced by the magnetic ordering below Néel temperature $T_N = 27.2$ K [4, 6].

At ambient pressure and $T = 4.2$ K, the values of isomer shift δ are about 0.31 and 0.39 mm/s in two sites, which corresponds to the high spin state of Fe^{3+} ions ($3d^5$, $S = 5/2$) in tetrahedral oxygen sites. At helium temperature, the values of magnetic hyperfine fields H_{hf} at iron nuclei in two sublattices are about 45.9 and 44.0 Tesla at ambient pressure, and the fields decrease as pressure is increased to 20 GPa (Fig. 2).

Relatively low values of H_{hf} (as compared with 55 T typical of iron oxides) can be explained by strong covalent bonding Fe–O in tetrahedral oxygen sites of the langasite structure, which leads to partial delocalization of $3d$ electrons thus decreasing the iron magnetic moment. Apparently, the compression of FeO_4 tetrahedra under pressure increases the Fe–O bonding leading to enhancement of the $3d$ delocalization, which in turn decreases the H_{hf} value. The $H_{hf}(P)$ behavior correlates with the decrease in the quadrupole splitting under pressure in the room temperature Mössbauer spectra (Fig. 3). However, at pressure above 20 GPa the field H_{hf} increases in both sublattices (Fig. 2), which can be associated with the structural transition observed by the high-pressure XRD studies at about 20 GPa [17, 24].

The temperature evolution of SMS spectra at different pressures is shown in Fig. 4. At $P < 20$ GPa, the six-line magnetic spectra gradually transform into a quadrupole doublet indicating transition to a paramagnetic state (Figs. 4b and 4c). Approaching the

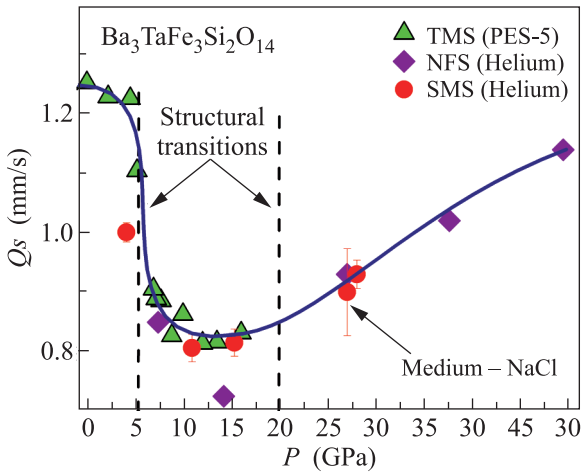

Fig. 3. (Color online) Pressure dependence of quadruple splitting parameter in langasite $Ba_3Ta^{57}Fe_3Si_2O_{14}$ at room temperature. Solid line is a guide for the eye.

Néel point T_N, coexistence of the magnetic and paramagnetic components can be seen in the spectra, which was not present at ambient pressure (Fig. 4a). Probably, this can be explained by some sample inhomogeneity produced by pressure. However, the temperature region of the coexistence of the magnetic and paramagnetic components is rather narrow, and the T_N values can be estimated with good accuracy. We found that at pressures $0 < P < 15$ GPa the T_N value only slightly increases from 27.2 to about 33 K (inset in Fig. 7a).

At pressures above the structural transition ($P > 20$ GPa), the temperature evolution of SMS spectra is very different from that at $P < 20$ GPa. The magnetically split component persists up to temperatures above 120 K (Fig. 5) indicating that a part of the sample has the T_N value increased by about four times! However, the area (fraction) of magnetic and paramagnetic components varies with temperature in a strange way (Figs. 5 and 6). As temperature is increased above 40 K, a paramagnetic doublet appears in the spectra on the background of magnetic sextet (Fig. 5). In region of 40–50 K, the paramagnetic fraction increases at the expense of magnetic component, however, between 50 and 115 K the fractions of magnetic and paramagnetic phases stabilize at the level of about 50/50%. Then, the magnetic fraction completely disappears at temperature of about 125 K.

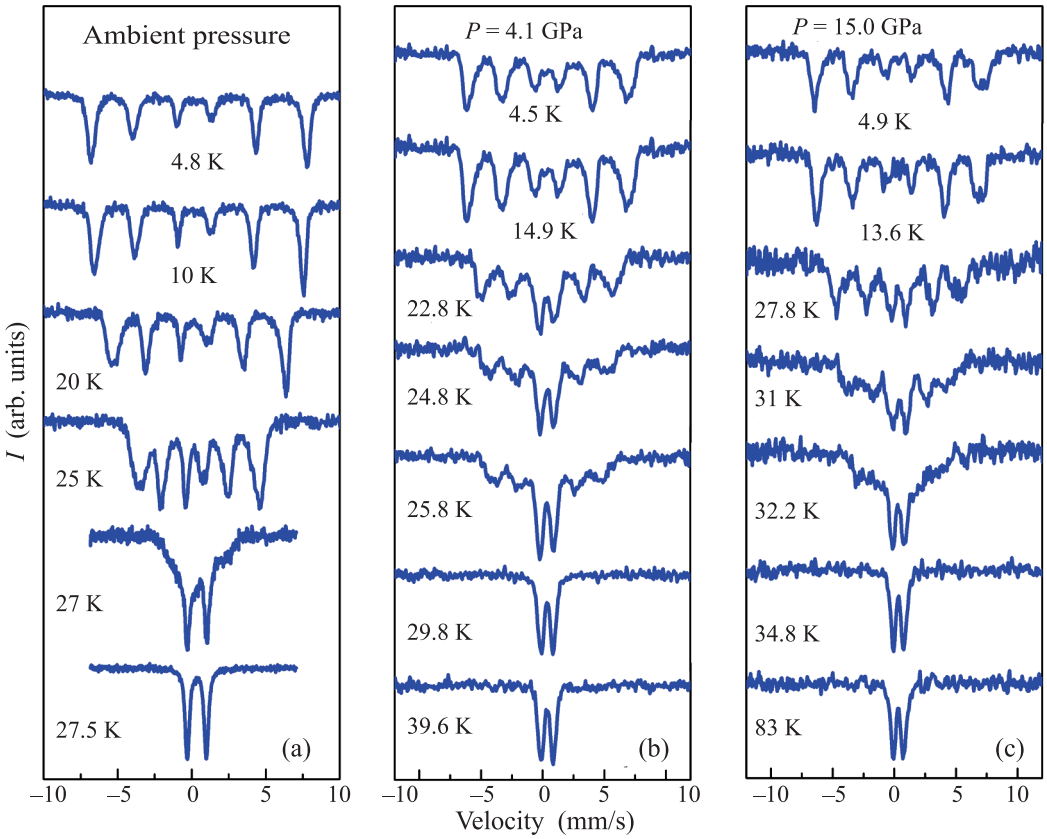

Fig. 4. (Color online) Evolution of SMS spectra with temperature in $Ba_3TaFe_3Si_2O_{14}$ at pressures below the structural transition at $P = 20$ GPa.

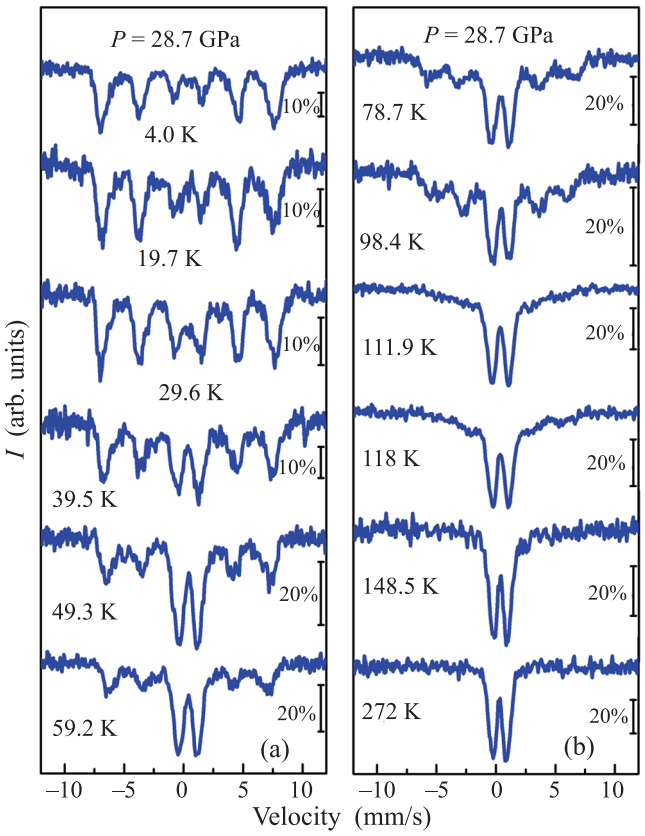

Fig. 5. (Color online) Evolution of SMS spectra with temperature in $Ba_3TaFe_3Si_2O_{14}$ at pressures above the structural transition at $P = 20$ GPa.

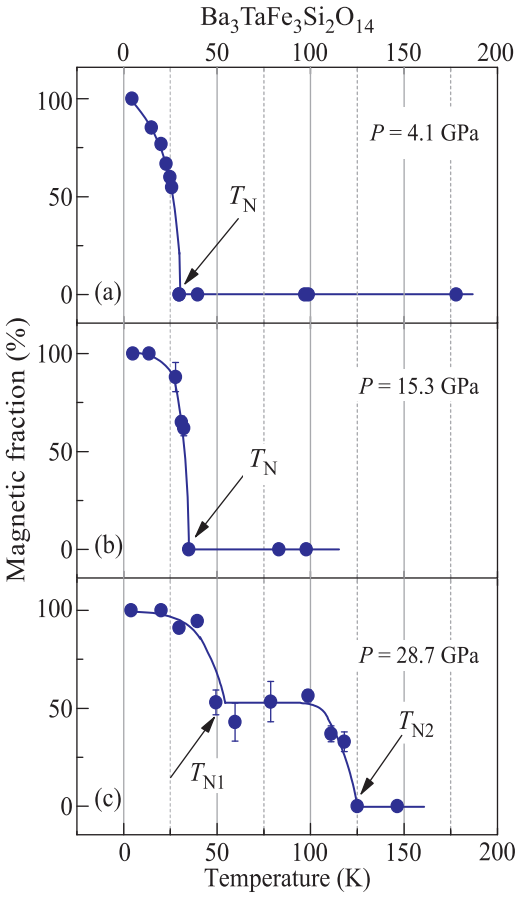

Fig. 6. (Color online) Temperature dependences of areas of magnetic (blue points) components in the Mössbauer spectra of $Ba_3TaFe_3Si_2O_{14}$ at different pressures below (a) and (b) and above (c) the structural transition at $P = 20$ GPa.

In Fig. 6, we plot the temperature dependences of contents of magnetic fraction of the sample at different pressure estimated from the areas of Mössbauer components. At $P < 20$ GPa, drastic transitions from the magnetically ordered to a paramagnetic state can be clearly seen by a sharp decrease in the magnetic fraction, and the precise value of T_N can be also obtained from such a presentation.

At pressures above 20 GPa, the coexistence of the magnetic and paramagnetic components is observed at temperatures extended up to about 125 K, but the temperature evolution is not smooth. At about 50 K, a half of iron ions transits from magnetic to paramagnetic state, and this temperature is indicated as T_{N1} in Fig. 6c. The other half of iron ions remains magnetically ordered up to about 125 K, and then it transits to a nonmagnetic state at about $T_{N2} = 130$ K (Fig. 6c). Two Néel temperatures observed imply a separation of the sample into two states with different magnetic properties.

In Fig. 7a, we plot the temperature dependences of average values of the magnetic hyperfine field $\langle H_{hf} \rangle$ at iron nuclei in the magnetic fraction of langasite $Ba_3TaFe_3Si_2O_{14}$ estimated from Mössbauer spectra at different pressures before and after the structural transition at 20 GPa. The T_N values obtained from the $\langle H_{hf} \rangle(T)$ behavior only slightly increases with pressure in the range of $0 < P < 20$ GPa (inset in Fig. 7a), but it significantly increases at $P > 20$ GPa (Fig. 7b).

4. DISCUSSION

It seems that a sample separation into two or even several phases with different magnetic properties takes place at $P > 20$ GPa. Most probably, a redistribution of iron ions between tetrahedral $3f$ and $2d$ sites or/and between tetrahedral $3f$ and octahedral $1a$ sites occurs as the result of structural phase transition at 20 GPa.

However, several reasons should be taken into account for explanation of such an effect:

(i) An effect of the sample inhomogeneous produced by pressure is unlikely since we used helium as hydrostatic pressure-transmitting medium. In addition, even when pressure medium is not ideally hydrostatic as helium (for example silicon oil) it cannot lead

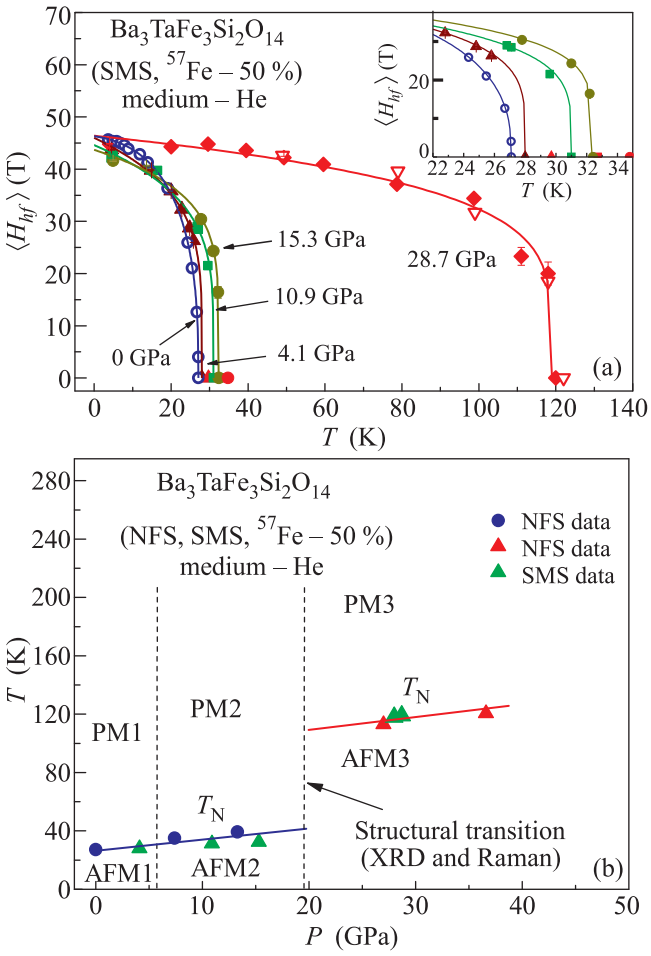

Fig. 7. (Color online) (a) Temperature dependences of the average values of magnetic hyperfine field $\langle H_{hf} \rangle$ at iron nuclei in the magnetic fraction of langasite $Ba_3TaFe_3Si_2O_{14}$ estimated from Mössbauer spectra at different pressures before and after the structural transition at 20 GPa. The inset shows the $\langle H_{hf} \rangle(T)$ dependences at $P < 20$ GPa in an enlarge scale. (b) Magnetic P–T phase diagram of langasite $Ba_3TaFe_3Si_2O_{14}$.

to such strong effect. Anyhow, the magnetic phase with high T_N value is present in this case.

(ii) At high pressure, the sample can be decomposed into small nanoclusters, which magnetic behavior is the similar to superparamagnetic properties of nanoparticles. Then, the temperature-transition to a paramagnetic state gradually proceeds through the relaxation of magnetic moments depending on the size of the clusters. In this case, the Mössbauer spectra should be significantly broadened into inner part of the spectrum, which was not observed in our experiments.

(iii) The high-spin to low-spin transition of Fe^{3+} ions should be taken into account. Appearance of the low-spin state ($S = 1/2$) will reduce the temperature of magnetic ordering of Fe^{3+} ions. However, this effect should be easily detected in the Mössbauer spectra by the changes in values of parameters of isomer shift and quadrupole splitting, which was not observed in our experiments.

In addition, the effect of HS ($S = 5/2$) $\rightarrow$ LS($S = 1/2$) spin-crossover in iron ions in tetrahedral sites of $Ba_3TaFe_3Si_2O_{14}$ is excluded because the energy of the LS term is very high at ambient pressure relative to the energy of the HS term. At pressure of about 20 GPa, the crystal field energy (spitted the e_g and t_{2g} levels of Fe^{3+}) is not high enough to compete with Hund energy of spin ordering [25]. Theoretical consideration [18] predicts much higher pressure value of the $HS \rightarrow LS$ spin-crossover transition for tetrahedral environment (about 800 GPa) in comparison with octahedral environment (about 70 GPa). Meanwhile, one of the possibilities of the spin-crossover is the structural transition with re-coordination of iron ions from tetra- to octa-environment of ligands.

(iv) In general, the redistribution of Fe^{3+} ions in langasite $Ba_3TaFe_3Si_2O_{14}$ at high pressures can occur either between two kinds of tetrahedral $3f$ and $2d$ sites (initially, the $2d$ sites are occupied by Si^{4+}) in the (ab) plane or/and between tetrahedral $3f$ and octahedral $1a$ sites (initially, the $1a$ sites are occupied by Ta^{5+}) in the nearest layers along the c axis. However, occupation of the octahedral sites by Fe^{3+} ions should change the Mössbauer parameters. In particular, the values of isomer shift δ and magnetic hyperfine field H_{hf} for the Fe^{3+} ions in the octahedral sites should be increased to about 0.45 mm/s and 55 T, respectively. Such an effect was not observed in our experiment. This implies that the redistribution of Fe^{3+} ions between the tetrahedral $3f$ and $2d$ sites in the (ab) plane is the most probable.

At ambient conditions, the Fe ion in $3f$ site (in the $Z \sim 1/2$ plane) has two nearest Si neighbors at $2d$ sites, while the Si ion in $2d$ site (in the $Z \sim 1/2$ plane) has three nearest Fe neighbors at $3f$ sites (Fig. 8).

As follows from the recent precise crystal structure refinement of $Ba_3TaFe_3Si_2O_{14}$ single crystals [12], the bond distances between cations and anions are: $Fe(3f) - O2(6g) = 1.904(3)$ Å; $Fe(3f) - O3(6g) = 1.850(2)$ Å; $Si(2d) - O1(2d) = 1.598(2)$ Å, and $Si(2d) - O2(6g) = 1.648(1)$ Å, while the bond angles are: $Fe(3f) - O2(6g) - Si(2d) = 133.1(1)$ grad and $Fe(3f) - Si(2d) - Fe(3f) = 119.88(1)$ grad.

At high pressure, the Fe^{3+} ions can be redistributed between the tetrahedral $3f$ and $2d$ sites as a result of the pressure-induced structural transition. In this case, superexchange interaction between Fe^{3+} ions in the nearest $3f$ and $2d$ sites passes through one oxygen at rather short Fe–O distances (of about 1.6–1.9 Å) and with the bond angle Fe–O–Fe of 133°. These

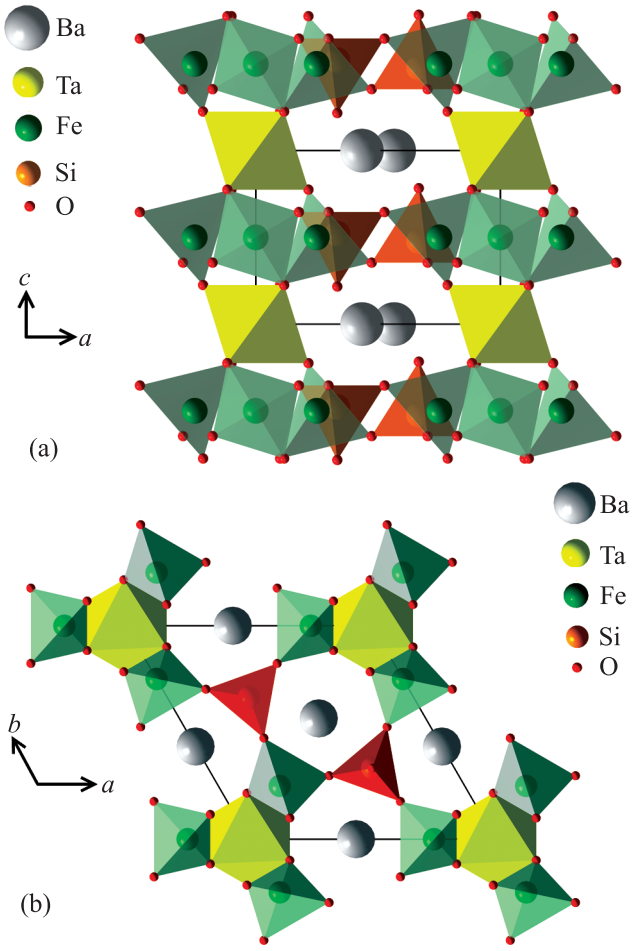

Fig. 8. (Color online) (a) a–c and (b) a–b projections of the trigonal crystal structure of langasite $Ba_3TaFe_3Si_2O_{14}$.

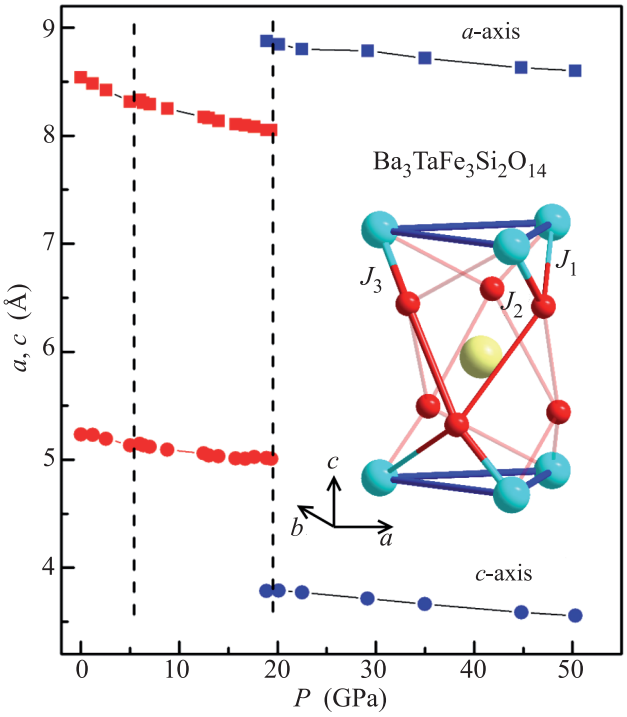

Fig. 9. (Color online) Unit cell parameters a and c versus the pressure in langasite $Ba_3TaFe_3Si_2O_{14}$. The inset shows the interlayer superexchange Fe–O–O–Fe interactions (J_1, J_2, J_3) between Fe^{3+} ions in the trigonal structure of $Ba_3TaFe_3Si_2O_{14}$.

exchange parameters are very effective for strong magnetic interaction between iron ions in the (ab) plane, and effective two-dimensional magnetic ordering can be expected in this case. Such strong interactions can essentially increase the magnetic transition temperature T_N, however, its value depends on the number of the Fe–O–Fe bonds for different local sites. In turn, this number depends on the probability of occupation of the 2d sites by Fe ions.

In general, if Fe and Si ions are randomly distributed over 3f and 2d sites, then the Fe ions in 3f site have three variants of the possible nearest neighbors in 2d sites (0Fe + 2Si), (1Fe + 1Si), and (2Fe + 0Si). The Fe ions in 2d site have four variants of the possible nearest neighbors in 3f sites (3Fe + 0Si), (2Fe + 1Si), (1Fe + 2Si), and (0Fe + 3Si).

In addition, one should take into account the next nearest neighbors of Fe with exchange interactions through two oxygen Fe–O–O–Fe, which realize both in ab plane and between adjacent ab planes along the c axis (Fig. 9).

The high pressures XRD studies of $Ba_3TaFe_3Si_2O_{14}$ revealed that at the structural transition at 20 GPa, the a unit cell parameter is increased, while the c parameter is greatly reduced [17]. The significant reduction of the c parameter should lead to a substantial increase in the Fe–O–O–Fe exchange interaction between adjacent ab planes, which can lead to an increase in the Néel point.

Thus, it can be suggested that the Néel temperature of $T_{N1} \approx 50$ K can be associated with the dominating role of the 2D magnetic ordering in the (ab) plane, while the value of $T_{N2} \approx 130$ K with the 3D magnetic ordering involving interplane interactions. The effect of magnetic state separation with two values of T_{N1} and T_{N2}, observed form the Mossbauer data, can indicate an appearance of magnetic superstructure in $Ba_3TaFe_3Si_2O_{14}$ langasite at pressures above 20 GPa. Considering the scenario for the redistribution of Fe and Si ions in the (ab) plane, this effect indicates that the distribution is not random, but some ordering of Fe ions at the 3f and 2d tetrahedral sites occurs in the high-pressure structure of the langasite. In the case of correlated occupation of the tetrahedral sites by Fe ions in neighboring (ab) layers the interplane interactions increase the T_N value.

5. CONCLUSIONS

The new method of synchrotron Mossbauer spectroscopy made it possible to perform very fine high-pressure experiments in DAC at low temperatures with the iron-containing langasite family crystals, which are now considered as a new class of promising multiferroics. Strong enhancement of the Néel temperature T_N revealed at high pressures is obviously associated with the structural transition at 20 GPa observed previously in our XRD studies [17]. The highest value of T_N is about 130 K which is almost five times larger than the value at ambient pressure (about 27 K).

It is supposed that the structural transition leads to distribution of the Fe^{3+} ions in both the 3*f* and 2*d* tetrahedral sites in the (*ab*) plane of the crystal. Analysis of the crystal structure indicated that the appearing Fe–O–Fe bonds are very effective for strong superexchange interaction between iron ions, and two-dimensional 2D magnetic ordering can be implemented in the (*ab*) plane.

In addition, as follows from the high pressures XRD studies of $Ba_3TaFe_3Si_2O_{14}$ [17], the significant reduction of the *c* parameter at pressures above 20 GPa should substantially increase the Fe–O–O–Fe exchange interaction between adjacent *ab* planes, leading to further increase in the Néel point. The revealed separation of the sample into two magnetic states with different T_N values of about 50 and 130 K can be explained by the dominating role of 2D magnetic ordering in the (*ab*) plane and 3D ordering involving interplane interaction.

The SMS measurements were performed at Nuclear Resonance beamline ID18 of ESRF. We deeply thank Dr. A.P. Dudka for providing the structural parameters of the $Ba_3TaFe_3Si_2O_{14}$ langasite and Dr. B.V. Mill' for fruitful discussions. The work was generally performed under support of the Russian Science Foundation (project no. 16-12-10464) and was supported by the Russian Foundation for Basic Research (project no. 17-02-00766) and by the Russian Ministry of Education and Science (contract no. 14.616.21.0068).

REFERENCES

1. B. V. Mill', E. L. Belokoneva, and T. Fukuda, Russ. J. Inorg. Chem. **43**, 1168 (1998).
2. B. V. Mill' and Y. V. Pisarevsky, in *Proceedings of the 2000 IEEE/EIA International Frequency Control Symposium and Exhibition, Kansas City, Missouri, 2000,* p. 133.
3. K. Marty, V. Simonet, P. Bordet, R. Ballou, P. Lejay, O. Isnard, E. Ressouche, F. Bourdarot, and P. Bonville, J. Magn. Magn. Mater. **321**, 1778 (2009).
4. I. S. Lyubutin, P. G. Naumov, and B. V. Mill', Eur. Phys. Lett. **90**, 67005 (2010).
5. K. Marty, P. Bordet, V. Simonet, M. Loire, R. Ballou, C. Darie, J. Kljun, P. Bonville, O. Isnard, P. Lejay, B. Zawilski, and C. Simon, Phys. Rev. B **81**, 054416 (2010).
6. I. S. Lyubutin, P. G. Naumov, B. V. Mill', K. V. Frolov, and E. I. Demikhov, Phys. Rev. B **84**, 214425 (2011).
7. S. A. Pikin and I. S. Lyubutin, Phys. Rev. B **86**, 064414 (2012).
8. H. D. Zhou, L. L. Lumata, P. L. Kuhns, A. P. Reyes, E. S. Choi, N. S. Dalal, J. Lu, Y. J. Jo, L. Balicas, J. S. Brooks, and C. R. Wiebe, Chem. Mater. **21**, 156 (2009).
9. H. D. Zhou, C. R. Wiebe, Y.-J. Jo, L. Balicas, R. R. Urbano, L. L. Lumata, J. S. Brooks, P. L. Kuhns, A. P. Reyes, Y. Qiu, J. R. D. Copley, and J. S. Gardner, Phys. Rev. Lett. **102**, 067203 (2009).
10. C. Stock, L. C. Chapon, A. Schneidewind, Y. Su, P. G. Radaelli, D. F. McMorrow, A. Bombardi, N. Lee, and S.-W. Cheong, Phys. Rev. B **83**, 104426 (2011).
11. E. L. Belokoneva and N. V. Belov, Sov. Phys. Dokl. **26**, 931 (1981).
12. A. P. Dudka, A. M. Balbashov, and I. S. Lyubutin, Crystallogr. Rep. **61**, 24 (2016).
13. A. P. Dudka, A. M. Balbashov, and I. S. Lyubutin, Cryst. Growth Des. **16**, 4943 (2016).
14. H. Narita, Y. Tokunaga, A. Kikkawa, Y. Taguchi, Y. Tokura, and Y. Takahashi, Phys. Rev. B **94**, 094433 (2016).
15. S. A. Pikin, I. S. Lyubutin, and A. P. Dudka, Crystallogr. Rep. **60**, 729 (2015).
16. I. S. Lyubutin and S. A. Pikin, J. Phys.: Condens. Matter. **25**, 236001 (2013).
17. I. S. Lyubutin, A. G. Gavrilyuk, Y. A. Davydova, A. G. Ivanova, I. A. Troyan, S. N. Sul'yanov, S. S. Starchikov, S. N. Aksenov, and K. V. Glazyrin, JETP Lett. **100**, 798 (2015).
18. A. G. Gavriliuk, I. S. Lyubutin, S. S. Starchikov, A. A. Mironovich, S. G. Ovchinnikov, I. A. Trojan, Y. Xiao, P. Chow, S. V. Sinogeikin, and V. V. Struzhkin, Appl. Phys. Lett. **103**, 162402 (2013).
19. A. G. Gavriliuk, A. A. Mironovich, and V. V. Struzhkin, Rev. Sci. Instrum. **80**, 043906 (2009).
20. V. Potapkin, A. I. Chumakov, G. V. Smirnov, R. Rüffer, C. McCammon, and L. Dubrovinsky, Phys. Rev. A **86**, 053808 (2012).
21. R. Rüffer and A. I. Chumakov, Hyperfine Interact. **97–98**, 589 (1996).
22. V. Potapkin, A. I. Chumakov, G. V. Smirnov, J.-P. Celse, R. Rüffer, C. McCammon, and L. Dubrovinsky, J. Synchrotr. Rad. **19**, 559 (2012).
23. C. Prescher, C. McCammon, and L. Dubrovinsky, J. Appl. Crystallogr. **45**, 329 (2012).
24. P. G. Naumov, V. Ksenofontov, I. S. Lyubutin, S. A. Medvedev, O. I. Barkalov, T. Palasyuk, E. Magos-Palasyuk, and C. Felser, Solid State Sci. **49**, 37(2015).
25. Y. Tanabe and S. Sugano, J. Phys. Soc. Jpn. **9**, 753 (1954).

SPELL: 1. cullet